Journal of NeuroVirology, 10: 387–399, 2004

ISSN: 1355-0284 print / 1538-2443 online
DOI: 10.1080/13550280490521131

Taylor & Francis
Taylor & Francis Group

Severe subcortical degeneration in macaques infected with neurovirulent simian immunodeficiency virus

JK Marcario,[1,4] KF Manaye,[5] KS SantaCruz,[2] PR Mouton,[6] NEJ Berman,[3,4] and PD Cheney[1,4]

Departments of [1]Molecular and Integrative Physiology, [2]Pathology and Laboratory Medicine, [3]Anatomy and Cell Biology, [4]Mental Retardation Research Center, University of Kansas Medical Center, Kansas City, Kansas, USA; [5]Department of Physiology and Biophysics, Howard University, Washington, DC, USA; [6]Department of Pathology, Laboratory of Experimental Gerontology, NIA/NIH, Johns Hopkins University Bayview Campus, Baltimore, Maryland, USA

Infection with human immunodeficiency virus-1 (HIV-1), the causative agent of acquired immunodeficiency syndrome (AIDS) in humans, causes a spectrum of neuropathology that includes alterations in behavior, changes in evoked potentials, and neuronal degeneration. In the simian immunodeficiency virus (SIV) model of HIV infection, affected monkeys show clinical symptoms and neurological complications that mimic those observed in human neuro-AIDS. To investigate the relationship between morphological correlates and neurophysiological deficits, unbiased stereology was used to assess total neuron number, volume, and neuronal density for all neurons in the globus pallidus (GP) and for dopamine (DA)-containing neurons in the substantia nigra (SN) in eight macaques inoculated with macrophage-tropic, neurovirulent SIV (SIVmac R71/17E), and five control animals. There was a significant difference between rapid progressors and controls for both neuron number ($P < .01$) and neuronal density ($P < .05$) in the GP, and for neuron number ($P < .05$) in the SN. Neuron loss ranged from 6% to 70% in the GP and from 10% to 50% in the SN. Neuropathological analyses confirmed neuroAIDS-like changes in brain, including microglial nodules, extensive perivascular cuffing and/or the presence of multinucleated giant cells, and alterations in neuronal morphology in the majority of the rapid progressors. By comparison, slow progressors showed little, if any, neuropathology. These neuropathological changes in SIV-infected monkeys indicate that neuron death and morphological alterations in the basal ganglia may contribute to the motor impairments reported in the SIV model and, by analogy, in the subset of patients afflicted with motor impairment in human neuro-AIDS. *Journal of NeuroVirology* (2004) **10,** 387–399.

Keywords: AIDS; basal ganglia; globus pallidus; motor; stereology; substantia nigra

Address correspondence to Joanne K. Marcario, PhD, Department of Molecular and Integrative Physiology, University of Kansas Medical Center, Mail Stop 1031, 3901 Rainbow Boulevard, Kansas City, KS 66160-7185, USA. E-mail: jmarcari@kumc.edu

Dr. Cheney is supported by NIH grants NDA12827 and HD02528. Funding for Dr. Mouton comes from the American Health Assistance Foundation, the Stereology Resource Center, and the U.S. Public Health Service. The authors would like to thank Dr. Leigh A.M. Raymond for sectioning the brains and thionin staining; Dr. Ravi Raghavan for the global neuropathological analyses; S. Mittal and S. Karra for tyrosine hydroxylase staining; and Dr. David Pinson for necropsy services.

Received 20 August 2003; revised 10 March 2004; accepted 23 July 2004.

Introduction

Human immunodeficiency virus (HIV) can infect the central nervous system (CNS) and lead to HIV-1–associated motor/cognitive disorder (Grant *et al*, 1995; Janssen *et al*, 1991; Seilhean *et al*, 1993) and acquired immunodeficiency syndrome (AIDS) dementia complex (Navia *et al*, 1986a, 1986b). AIDS dementia complex is a serious, disabling disease characterized by cognitive, behavioral, and motor dysfunctions. Basal ganglia involvement in HIV-1 infection may contribute to the psychomotor symptoms

associated with HIV dementia (Bansal *et al*, 2000). Berger and Nath (1997) have noted that HIV infection frequently results in a dementing illness that manifests as a subcortical dementia, including degeneration of the dopaminergic nigrostriatal pathway. Parkinsonism appears prominent in these patients and may be part of the initial presentation of symptoms. Furthermore, the motor dysfunction in these patients responds well to dopaminergic blocking agents. To date, however, no studies in experimental animals have established strong clinicopathological relationships between HIV-1–mediated neuropathology and degree of neural system impairment.

Neuronal pathology associated with HIV infection has been demonstrated in both subcortical and cortical brain regions at autopsy. Using unbiased stereological techniques, Subbiah *et al* (1996) demonstrated that AIDS patients, particularly those with HIV-associated dementia, show significant cortical atrophy compared to seronegative controls. A global neuronal loss of 37% throughout all four neocortical lobes was reported by Oster *et al* (1995). Everall *et al* (1995) reported neuronal loss in the putamen and Reyes *et al* (1991) showed a decrease in the number of cell bodies in the substantia nigra.

Infection of macaques with neurovirulent strains of simian immunodeficiency virus (SIV_{mac}) reveals several aspects of the neurological disease observed in humans with HIV infection, though over a shorter time course. Neurovirulent SIV_{mac} inoculation in macaques results in persistent infection with early infection of the CNS. We have previously reported behavioral deficits (Marcario *et al*, 1999a, 1999b) and neurophysiological abnormalities (Raymond *et al*, 1999, 2000) in a cohort of nine monkeys infected with neurovirulent strains of SIVmac. Deficits in a motor skill task were observed (Marcario *et al*, 1999a), and the majority of monkeys developed ataxia and/or tremor following inoculation. Motor-evoked potential studies showed increased latency and increased central conduction time (Raymond *et al*, 1999). Global neuropathological changes assessed by histological examination of these same animals revealed HIV-like microglial nodules, multinucleated giant cells, and perivascular cuffing (Raghavan *et al*, 1999).

To investigate the association between neuronal loss and motor system deficits in the SIV model, we used modern stereological approaches (Mouton, 2002) to quantify neuronal changes in the globus pallidus (GP) and substantia nigra (SN). In addition, neuropathological changes characteristic of neuro-AIDS were assessed by histological examination. We hypothesize that neuronal loss in the basal ganglia will correlate well with neuropathology in these structures, and with other measures of CNS function on which we have previously reported.

Results

We examined the brains of 13 macaques: 5 uninoculated adolescent male controls, and 8 adolescent male macaques inoculated with a cocktail of neurovirulent SIV of viruses R71 and 17E. Of the eight inoculated macaques, six were rapid progressors, and two were slow progressors. Analysis of the SN of AQ12 was not possible because the entire nucleus was not present in all sections of the series to be counted. So, for all analyses in the GP, $n = 6$ for the rapid progressors and $n = 2$ for the slow progressors; in the SN, $n = 5$ for the rapid progressors and $n = 2$ for the slow progressors. It should also be noted that only tyrosine hydroxylase (TH)-positive neurons were evaluated in the SN (Table 1).

There were two rapid progressors that showed little neuron loss compared to the other rapid progressors (AQ12 in the GP and AQ38 in the SN). We did notice, however, that these animals still showed severe neuropathology in the GP and moderate neuropathology in the SN. There were also very noticeable changes in neuronal morphology, such as absent dendrites and changes in soma shape, in both the GP and the SN of both animals. We therefore contend that although these animals had "countable" neurons, these neurons were not functionally viable. As such, we have decided to analyze the data both with and without these animals. Both sets of results are presented.

Table 1 Severity of neuropathology and motor system impairment for eight SIV-infected monkeys

Monkey	*Disease progression*	*Weeks survived*	*GP neuropathology*[1]	*SN neuropathology*[1]	*Motor system neuropathology*[2]	*Motor evoked potential changes*[2]
AQ70		14	Mild	Mild	Mild	Severe
AQ69		9	Mild	None	N/A	Mild
AQ43		6	Very Severe	Moderate	Severe	Severe
AQ12	Rapid	14	Severe	Moderate	Moderate	Moderate
AQ38		7	Moderate	Moderate	Severe	Severe
AQ20		8	Mild	None	Mild	Mild
AQ15	Slow	109	None	None	Mild	None
AQ94		87	None	None	None	None

[1]Neuropathology is rated on a scale from 0 to 4: 0 = none; 1 = mild; 2 = moderate; 3 = severe; 4 = very severe.
[2]Data from Raymond *et al*, 1999.

Neuron number
The mean number of neurons in the GP of control macaques was 714,775 (±67,544). The mean number of neurons in the six SIV-infected rapid progressors examined was 421,033 (±56,976). This represents a 41% neuron loss and a statistically significant change from controls ($P < .01$). When the results were analyzed without AQ12, the outcome changed only slightly (46% neuron loss, $P < .01$). The mean number of neurons in the two SIV-infected slow progressors was 608,602 (±48,592), a 15% neuron loss.

The mean number of TH-positive neurons in the SN of control macaques was 406,482 (±45,344). The mean number of TH-positive neurons in the five SIV-infected rapid progressors examined was 293,199 (±39,488). This represents a 28% neuron loss, which is significantly less than the number of neurons in the controls ($P < .05$). When the results were analyzed without AQ38, there was a greater group effect (36% neuron loss, $P = .02$). This should be expected, as AQ38 actually had 4% more neurons than the control group mean, thus driving up the average number of neurons for the rapid progressors. The mean number of TH-positive neurons in the two SIV-infected slow progressors was 344,557 (±21,289), which represents a 15% neuron loss (Figure 1A).

Region volume
The mean volume of the GP for control macaques was 229 mm^3 (±13). The mean volume of the GP for the SIV-infected rapid progressors examined was 213 mm^3 (±12), only 7% less than controls ($P = .33$), which was not a significant difference. When the results were analyzed without AQ12, the loss in volume remained at 7% ($P = .42$). The mean volume of the GP in the two SIV-infected slow progressors was 227 mm^3 (±5), which represents a 1% volume loss.

The mean volume of the SN of control macaques was 348 mm^3 (±23). The mean volume of the SN for the five SIV-infected rapid progressors examined was 291 mm^3 (±48); a 16% volume loss compared to controls ($P = .42$), which was not significant. When the results were analyzed without AQ38, there was a greater decrease in volume, 27% ($P = .11$), although still not statistically significant. The mean volume of the SN in the two SIV-infected slow progressors was 363 mm^3 (±12), 4% less than controls (Figure 1B).

Neuronal density
The mean neuronal density of the GP for control macaques was 3134 neurons/mm^3 (±263). The mean neuronal density of the GP for the SIV-infected rapid progressors examined was 2034 neurons/mm^3 (±312), 35% less than controls ($P = .03$), a significant difference. When the results were analyzed without AQ12, the outcome changed only moderately, 40% less than controls ($P = .02$), which was still a significant difference. The mean neuronal density of the GP in the two SIV-infected slow progressors was 2692 neurons/mm^3 (±268), which represents a 14% loss in neuronal density.

The mean neuronal density of TH-positive neurons in the SN of control macaques was 1159 neurons/mm^3 (±72). The mean neuronal density of TH-positive neurons in the SN for the five SIV-infected rapid progressors examined was 1033 neurons/mm^3 (±67), an 11% loss of neuronal density compared to controls ($P = .31$), which was not significant. When the results were analyzed without AQ38, the mean decrease in neuronal density was 10%, which was also not significant ($P = .41$). The mean neuronal density of TH-positive neurons in the SN in the two SIV-infected slow progressors was 949 neurons/mm^3 (±28), 18% less than controls (Figure 1C).

Neuropathology
Neuropathological changes were evaluated in the right hemisphere using thionin-stained tissue. Evidence of typical retroviral induced CNS neuropathology was observed in the majority of animals from which tissue was available (Figure 2). Neuropathological findings consisted of perivascular cuffing, meningitis, microglial nodule formation, multinucleated giant cell reactions, and perilesion axonal degeneration caused by white matter inflammatory lesions. The severity of pathology varied from animal to animal (see Figure 2). Ratings reflecting the severity of neuropathology in both the GP and SN are given in Table 1. Neither of the slow progressors (AQ15 and AQ94) showed any neuropathology in the GP or the SN. The rapid progressors showed mild (AQ70, AQ20, AQ69), moderate (AQ38), severe (AQ12), and very severe (AQ43) neuropathology in the GP, including inflammatory foci and multinucleated giant cells. In the SN, two rapid progressors showed no neuropathology (AQ20 and AQ69), and the rest showed mild (AQ70) to moderate (AQ38, AQ43, AQ12) neuropathology. In general, perivascular cuffing was present in both mild and severe cases, whereas multinucleated giant cells were found only in severe cases.

Neurological analysis
Ataxia, tremor, and weakness were determined by daily observation before and during behavioral testing, and as seen in weekly home cage behavior tapes. In addition, periodic neurological evaluations were performed, in which grip strength, gait, and climbing ability were assessed qualitatively. Four of six rapid progressors (67%) showed signs of muscular weakness and loss of grip strength, three of six (50%) showed evidence of tremor, and five of six (83%) showed evidence of ataxia.

Correlations
Pearson correlation coefficients (ρ) were calculated based on the severity ratings for the number of weeks

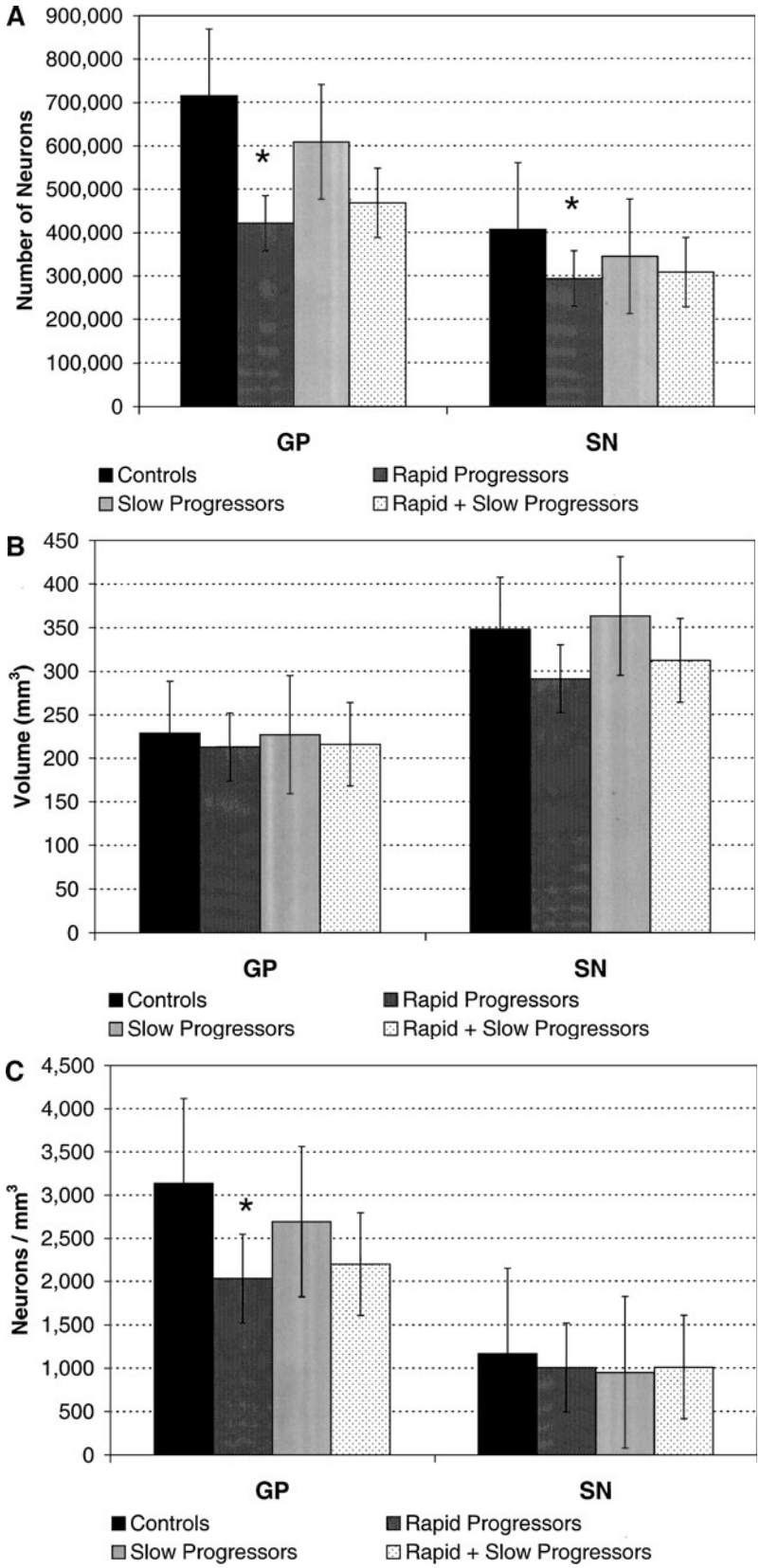

Figure 1 Stereological analysis of the GP and SN. (**A**) Number of neurons in the rapid progressors was significantly different from the control means in both the GP and SN. One animal (AQ38) had a 70% loss of neurons in the GP. In the SN, AQ70 had the greatest neuronal loss (47%). (**B**) Volume was not significantly different from control means for the rapid progressors in either the GP or the SN. (**C**) Neuronal density in the rapid progressors was significantly different from control means in the GP, but not the SN. The asterisk (*) denotes significant differences from control means. The error bars in each data series represent the standard error of the mean.

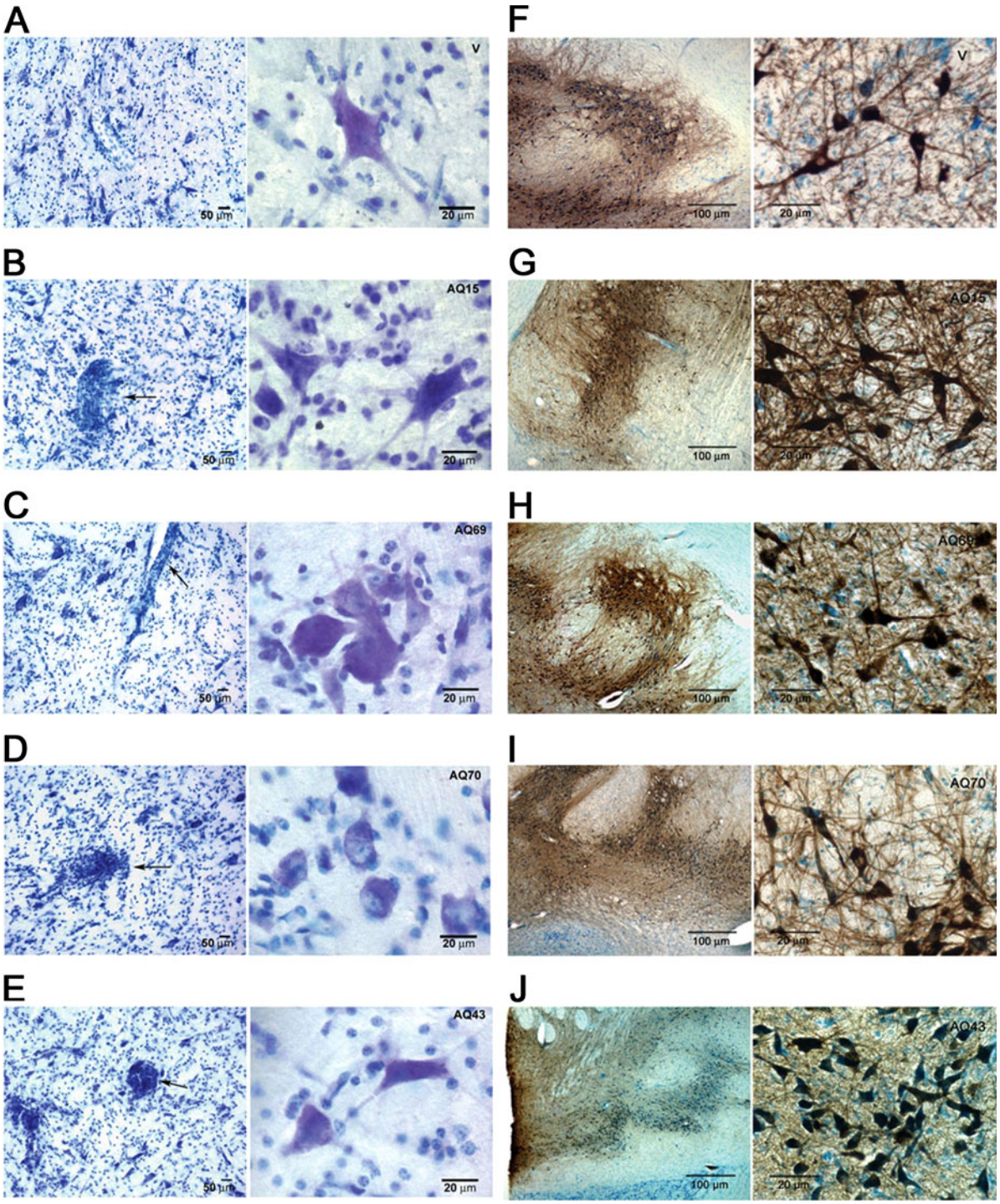

Figure 2 Neuropathology and changes in neuronal morphology in the GP and SN of SIV-infected rhesus macaques. In each row, the panel from the GP and the panel from the SN are from the same animal. *Left column*: Thionin-stained sections from the GP. (**A**) Control animal V—no neuropathology; normal neuronal morphology and normal blood vessels and surrounding cells. (**B**) Slow progressor AQ15—very mild neuropathology, consisting mainly of light perivascular cuffing (*arrow*), and normal neuronal morphology. (**C**) Rapid progressor AQ69—mild neuropathology, consisting mainly of perivascular cuffing (*arrow*) with some inflammatory foci. Most neurons appear similar to those of controls, but there is rounding of the soma and shortening of the dendrites of some neurons. (**D**) Rapid progressor AQ70—moderate neuropathology, consisting of microglial nodules (*arrow*), perivascular cuffing, and other inflammatory foci. Many of the neurons show a loss of dendrites, decreased staining in the cytoplasm, and a round soma. (**E**) Rapid progressor AQ43—severe neuropathology, consisting of perivascular cuffing, multiple inflammatory foci, microglial nodules, and a multinucleated giant cell (*arrow*, as seen in thick sections). Some neurons appear similar to those of controls, others show altered neuronal morphology, such as lack of dendrites. *Right column*: Thionin- and tyrosine hydroxylase (TH)-stained sections from the SN. (**F**) Control animal V—no neuropathology, dense terminal field. (**G**) Slow progressor AQ15—no neuropathology, dense terminal field. (**H**) Rapid progressor AQ69—very mild neuropathology, most neurons similar to those in controls. (**I**) Rapid progressor AQ70—mild neuropathology, most neurons similar to controls. (**J**) Rapid progressor AQ43—moderate neuropathology, very sparse terminal field, some abnormalities in neuronal morphology, such as loss of dendrites.

Table 2 Correlation coefficients (ρ) for the globus pallidus and substantia Nigra

Rapid progressors + slow progressors	*Weeks survived*[1]	*Motor EP changes*[2]	*Motor system neuropath*[2]	*GP neuropath*	*GP neuron loss*	*SN neuropath*	*SN DA neuron loss*	*Ataxia*[1]
Weeks survived	1.00							
Without AQ38 and AQ12								
Motor-evoked potential changes	− 0.76	1.00						
Without AQ38 and AQ12	− 0.76							
Motor system neuropathology	− 0.58	0.77	1.00					
Without AQ38 and AQ12	−0.58	0.77						
GP neuropathology	− 0.66	0.74	0.85	1.00				
Without AQ38 and AQ12	− 0.66	0.74	0.85					
GP neuron loss	− 0.76	0.65	0.65	0.49	1.00			
Without AQ38 and AQ12	− 0.87	0.72	0.76	0.73				
SN neuropathology	− 0.54	0.84	0.88	0.87	0.37	1.00		
Without AQ38 and AQ12	− 0.54	0.84	0.88	0.87	0.61			
SN DA neuron loss	− 0.50	0.50	0.08	0.49	0.23	0.26	1.00	
Without AQ38 and AQ12	− 0.76	0.93	0.56	0.71	0.52	0.79		
Ataxia	−0.64	0.89	0.85	0.86	0.40	0.97	0.39	1.00
Without AQ38 and AQ12	−0.64	0.89	0.85	0.86	0.63	0.97	0.91	

[1]Data from Marcario *et al*, 1999a.
[2]Data from Raymond *et al*, 1999. Motor system structures examined: motor cortex, basal ganglia, cerebral peduncles, long white tracts, peripheral nerve.

survived, motor evoked potential changes, motor system neuropathology, GP neuropathology, GP neuron loss, SN neuropathology, SN dopamine (DA)-containing neuron loss, and ataxia using the data from all six rapid progressors and both slow progressors (Table 2). The data for motor system neuropathology (which included the motor cortex, basal ganglia, cerebral peduncles, long white tracts, and some peripheral nerves) and motor-evoked potential changes were taken from Raymond *et al*, 1999. The data for the ataxia were taken from Marcario *et al*, 1999a, and are discussed in depth in that paper. All of these data were collected from the same six rapid progressors. The correlations we performed have been calculated to highlight the relationship between those data presented in the aforementioned studies, and the data from the current study.

There was a moderate to strong inverse correlation between survival time and all other measures; animals with greater neuropathology, neuron loss, or changes in motor-evoked potentials had shorter survival times. Motor-evoked potential changes were strongly correlated with motor system neuropathology ($\rho = 0.77$), GP neuropathology ($\rho = 0.74$), and SN neuropathology ($\rho = 0.84$); they were moderately correlated with GP neuron loss ($\rho = 0.65$) and SN neuron loss ($\rho = 0.50$). Motor system neuropathology was most strongly correlated with GP ($\rho = 0.85$) and SN ($\rho = 0.88$) neuropathology, moderately with GP neuron loss ($\rho = 0.65$), and poorly with SN neuron loss ($\rho = 0.08$). GP neuropathology was most strongly correlated with SN neuropathology ($\rho = 0.87$), and moderately with both GP ($\rho = 0.49$) and SN ($\rho = 0.49$) neuron loss. SN neuropathology was weakly correlated with both GP ($\rho = 0.37$) and SN ($\rho = 0.26$) neuron loss. Finally, GP neuron loss was only weakly correlated with SN neuron loss ($\rho = 0.23$).

Correlations were also performed between the severity of ataxia that was qualitatively observed in each animal, and each of the other factors previously mentioned (see Table 2). There were very strong correlations between ataxia and motor EP changes ($\rho = 0.89$), motor system neuropathology ($\rho = 0.85$), GP neuropathology ($\rho = 0.86$), and SN neuropathology ($\rho = 0.97$). Moderate correlations were also obtained between ataxia and GP neuron loss ($\rho = 0.40$), SN neuron loss ($\rho = 0.39$), and the number of weeks the animal survived ($\rho = 0.64$).

We have contended that the low level of neuron loss in the GP of AQ12 and in the SN of AQ38 should be considered outlier values because of the abnormal morphological characteristics of the neurons observed in these areas (i.e., the neurons appear damaged but are still "countable"). If we exclude the severity ratings of AQ12 for GP neuron loss, the strength of the correlations with all other measures increase in magnitude: from strong to very strong for survival time ($\rho = -0.76$ to $\rho = -0.87$); from moderate to strong for motor-evoked potential changes ($\rho = 0.65$ to $\rho = 0.72$), motor system neuropathology ($\rho = 0.65$ to $\rho = 0.76$), and for GP neuropathology ($\rho = 0.49$ to $\rho = 0.73$); from weak to moderate for SN neuropathology ($\rho = 0.37$ to $\rho = 0.61$) and SN neuron loss ($\rho = 0.23$ to $\rho = 0.52$); and, although both values were moderate, there was an increase for ataxia ($\rho = 0.40$ to $\rho = 0.63$). If we exclude the severity ratings of AQ38 for SN neuron loss, the strength of the correlations with all other measures increases in magnitude: from moderate to strong for survival time ($\rho = -0.50$ to $\rho = -0.76$); from moderate to very strong

for motor-evoked potential changes ($\rho = 0.50$ to $\rho = 0.93$); poor to moderate for motor system neuropathology ($\rho = 0.08$ to $\rho = 0.56$); from moderate to strong for GP neuropathology ($\rho = 0.49$ to $\rho = 0.71$); from weak to strong for SN neuropathology ($\rho = 0.26$ to $\rho = 0.79$); and from weak to moderate for GP neuron loss ($\rho = 0.23$ to $\rho = 0.52$); and from moderate to very strong for ataxia ($\rho = 0.39$ to $\rho = 0.91$).

Discussion

In this study, we set out to determine whether in SIV-infected rhesus macaques, there was neuron loss and neuropathology in the basal ganglia similar to that reported in the human clinical literature. We have shown that productive infection in the brain is accompanied by inflammatory foci and by loss of neurons in motor-related areas of the brain. The loss of neurons in the GP and the loss of DA-containing neurons in the SN of these animals did correlate with abnormalities in motor-evoked potentials and motor system neuropathology. These results also demonstrate the power of unbiased stereological techniques in establishing neuron loss in this animal model of neuroAIDS.

Neuron number
Compared to controls, most SIV-infected animals showed significant neuron losses in the GP of greater than 25%, with some exceeding 50%. We also examined whether DA-containing neurons are lost in the SN, by staining sections with TH and counterstaining with 1% thionin. Compared to controls, three of five SIV-infected animals showed significant neuron losses in the SN of greater than 30%.

Infection with HIV-1 is often associated with neuronal loss in subcortical and cortical regions. This loss may appear clinically as motor dysfunction and/or dementia. Supporting results have been reported in humans infected with HIV-1. Using unbiased stereological probes, Fischer *et al* (1999) found significant neuron loss throughout the frontal, temporal, parietal, and occipital cortices, with greater loss of large versus small neurons. Using morphometric analyses, Itoh *et al* (2000) found a significant decrease in the total number of neurons in the SN, and a significant decrease in the number of pigmented neurons compared to controls. Further, using high-resolution magnetic resonance spectroscopy (MRS) and quantitative neuropathology, Gonzalez *et al* (2000) found losses in n-acetylaspartate and calbindin in frontal cortical gray matter, which indicated neuronal injury and/or death. Finally, Lopez *et al* (1999) have noted that HIV has a propensity to invade subcortical CNS areas, particularly the basal ganglia, and have found that damage to DA-containing neurons seems to occur early in the disease course. HIV-associated dementia (HAD) patients had decreased levels of cerebrospinal fluid (CSF) DA, and a reduction of the DA metabolite homovanillic acid, but a relative preservation of other neurotransmitters, which suggests a preferential loss of DA neurons. Neuropathologic analysis showed neuron loss in the GP, and less severe loss in the neocortex. Taken together, these findings suggest that there is ample evidence to support the loss of neurons in both cortical and subcortical areas in a number of different HIV-1 model systems.

We have observed tremor, ataxia, and other neurological symptoms in our animals that are similar to those that can be attributable to the "subcortical dementias." The neuron loss observed in this study and the corroborating evidence of the motor-evoked potential abnormalities strongly suggests that DA neurons are lost in the SN of SIV-infected primates. However, it is possible that the loss of DA neurons we observed was due to a cessation of DA production by neurons in the SN. Those neurons would not have been visualized with the TH stain, thus not counted. In our study, however, because total neuron number in the SN using thionin-only-stained sections was not examined, it is not know whether or not this is the case. This possibility will be investigated in future work.

Structure volume and neuronal density
In our studies, there was no significant change in the volume of either the GP or SN in any of the SIV-infected monkeys, compared to controls. This is in contrast to some neuropathological studies of patients with AIDS in which there is a reduction in neocortical and subcortical structure volumes. Using stereological techniques, Oster *et al* (1993) found a reduction in the mean volume of the neocortex and the central brain nuclei in patients with AIDS, and Subbiah *et al* (1996) showed that there was a significant reduction in mean neocortical volume in AIDS patients, compared to seronegative controls. Using magnetic resonance imaging (MRI) techniques, Aylward *et al* (1993) found that HIV+ demented patients had smaller basal ganglia volumes than either the nondemented or control groups.

Our results do show a significant decrease in neuronal density of approximately 35% in the GP, and a mean decrease in neuronal density of approximately 11% in the SN, compared to controls. This finding is supported by other studies of human AIDS patients. Everall *et al* (1995) found a 21% decrease in neuronal density in the putamen of nondemented patients that had died of AIDS. Earlier, this same group of researchers had found that neuronal density in the frontal cortex was significantly lower in HIV versus control subjects (Everall *et al*, 1991). Further, Ketzler *et al* (1990) found a significant loss of neurons and an 18% loss in neuronal density in the fronto-orbital cortex of AIDS patients versus controls.

Neuropathological data
In our studies, large, disseminated microglial nodules, inflammatory foci, and extensive perivascular

cuffing were found in the GP, and to a lesser extent in the SN, of rapid progressors. Multinucleated giant cells were also found in the GP of three of the rapid progressors. Neither of the slow progressors showed any overt neuropathology in the GP or the SN. The neuropathology we observed was very similar to the hallmark neuropathology observed in the postmortem examination of the brains of AIDS patients. However, there was not always a strong correlation between neuron loss and the severity of neuropathology found in GP and the SN, as was evidenced in AQ12 and AQ38. Although these animals had severe neuropathology, they did not have a corresponding neuron loss.

It has been widely reported, in the human clinical literature, that dementia can occur in endstage AIDS in the absence of overt neuropathology and that considerable pathology may exist in the absence of dementia (Everall *et al*, 1994; Glass *et al*, 1993). One of the conclusions drawn from a number of studies is that the magnitude of neuron loss does not correlate with the degree of cognitive dysfunction or dementia exhibited by HIV+ patients (Weis*et al,* 1993; Everall*et al,* 1994). A number of motor skill studies in the human literature have reported motor dysfunction in HIV-infected patients in the absence of clinical symptoms and contend that fine motor control deficits are detectable prior to the development of other major manifestations of HIV infection (Arendt *et al*, 1990, 1993, 1994). Finally, Murray *et al* (1992) reported that in some monkeys infected with SIV_{smm} Delta B670, neuropathology was limited despite the presence of significant cognitive and/or motor deficits.

Such findings suggest that although the neuropathology found in the brains of the rapid progressors may contribute to the motor-evoked potential changes and the clinical neuropathological symptoms we observed, functional injury may precede the appearance of noticeable pathology and neuronal death. It is possible that functional injury to neurons may be much more widespread than actual overt neuropathology or neuronal cell death and that it may contribute significantly to functional impairment. This is why we chose to report our observations of changes in neuronal morphology even though we were not able to quantify the magnitude of those changes at this time.

Relation to motor-evoked potentials (MEPs)

We used transcranial electrical stimulation of motor cortex and the spinal cord to assess motor system function on the same animals we used for the neuropathological analyses in this study (see Raymond *et al*, 1999, for detailed results). Five of the six rapid progressors we examined for neuron loss showed postinoculation latency increases in at least one cortical MEP and all six showed postinoculation latency increases in at least one spinal cord MEP (peripheral conduction time). Increases in central conduction time (CCT) were evident in four of six rapid progressors. Neither of the slow progressors showed significant latency increases in either cortical or spinal cord MEPs or CCT. The correlational analyses performed in this study showed strong to very strong correlations between extent of MEP abnormalities and the presence of classic HIV/SIV neuropathology in the GP, SN, and motor system as a whole. There was a moderate correlation between MEP abnormalities and neuron loss in both the GP and SN. In addition, there was a strong correlation between MEP abnormalities and the number of weeks an animal survived (see Table 2).

These results support our contention that motor system structures, and the basal ganglia in particular, are targets of SIV infection. A few studies in the human clinical literature also support this conclusion. Moglia *et al* (1991) found altered MEPs, mostly due to a prolongation of the central motor conduction time in HIV-seropositive versus-seronegative patients. Similarly, Somma-Mauvais and Farnarier (1992) found that MEPs by magnetic stimulation reveal prolonged central motor conduction time in 46% of HIV+ asymptomatic subjects.

Alterations in neuronal morphology; dendritic, synaptic, and axonal damage

In these studies, we identified two animals (AQ12 and AQ38) that were considered to be "clinical outliers" because the difference between their neuronal counts and those of the rest of the rapid progressors differed by more than 1.5 standard deviations. If we exclude the severity ratings for AQ12 regarding GP neuron loss, and from AQ38 regarding SN neuron loss, the strength of the correlation with all other measures increases in magnitude. These animals had little neuronal loss, but had clearly abnormal dendritic morphology. Although we were not able to quantify the magnitude of dendrite loss and did not quantitatively rate the alterations in neuronal morphology, we believe it was important to note the changes observed, because they may be indicative of dendrite/axon damage or changes in the functionality of neurons.

One weakness of the stereological methods used is that they do not take into account the functionality of neurons. Neurons that had mostly intact cell membranes and a visible nucleus were counted, the same as "normal" looking neurons were, even if they showed evidence of morphological alteration, or lacked dendrites and axons. These two rapid progressors did show severe neuropathology and did develop ataxia and/or tremor.

It has been suggested that widespread synaptic and/or dendritic injury may be involved in the neurological impairment and clinical symptoms that occur in HIV-1 infection. Everall *et al* (1999), found a significant correlation between reduced synaptic density and poor neuropsychological performance in AIDS patients. They concluded that a combination of factors, including synaptic damage, specific

neuronal loss, and increasing viral load underlies HIV-associated cognitive impairment. Using MRS and quantitative neuropathology, Gonzalez *et al* (2000) have found decreases in synaptophysin immunoreactivity in frontal cortical gray matter, indicating synaptodendritic injury. Also, a study using beta-amyloid precursor protein (beta-APP) immunostaining as a marker found evidence of axonal damage in both asymptomatic and symptomatic HIV+ individuals (An *et al*, 1997).

In a rhesus macaque model of HIV infection, Li *et al* (1999) found that productive infection of cells of the macrophage lineage in the CNS is associated with inflammation, increased expression of inducible nitric oxide synthase (iNOS) and dendritic injury, and concluded that increased NO accompanying productive infection and encephalitis may be one cause of neuronal injury in SIV infection. A recent study by Mankowski *et al* (2002) found that beta-APP accumulation in the white matter (corpus callosum) of SIV-infected macaques develops during SIV infection, in close correlation with levels of viral replication and may serve as a sensitive marker of neuronal/axonal damage mediated by viral proteins.

Conclusions

The progression of human neuro-AIDS can be effectively modeled, over a relatively short time course, using monkeys infected with neurovirulent SIV. Previously reported studies have shown that behavioral deficits and clinical signs in monkeys resemble those found in HIV-infected humans. The disease course of the SIV-infected macaques in this study took two distinct routes; six monkeys exhibited a rapid disease progression, whereas the other two experienced a much slower disease progression. The results presented in this study show profound neuron loss in the GP and a lesser loss in the DA-containing neurons of the SN of rapid progressors, compared to controls, and significantly reduced neuronal density in the GP. Neuropathology was particularly evident in the GP, including perivascular cuffing, multiple inflammatory foci, and evidence of multinucleated giant cells in three animals. Many of these same neuropathological findings were evident in the SN, though not as severe as in the GP. Slow progressors did not show large changes in neuron number, minimal neuropathology, minimal alterations in neuronal morphology, and no signs of ataxia.

Although neuron loss was prominent in most of the rapid progressors, AQ12 and AQ38 had severe neuropathology, but did not have a corresponding neuron loss. However, these two animals did show changes in neuronal morphology that were greater than the changes found in some of the other rapid progressors. Alterations in neuronal morphology and dendritic pathology may provide a potential explanation for the observed clinical neurological symptoms and MEP irregularities in the rapid progressors, and in AQ12 and AQ38 in particular. Dendritic and synaptic damage without frank neuronal loss may be seen in milder HIV-related cognitive disorders.

Thus, it seems that in addition to the standard postmortem neuropathological assessments now performed, neuronal counting methods based on stereology may be needed to supplement standard neuropathological analyses to more accurately describe the biological basis for observed AIDS-related motor and cognitive impairments. Further, loss of dendrites and other changes in neuronal morphology may need to be investigated more rigorously as possible factors underlying behavioral and neurological causes for neurophysiological deficits. Synapse volume estimates, performed by stereological methods, could enhance the ability to detect subtle changes that may accompany cognitive impairment in HIV infection. As synaptic damage is potentially reversible, early diagnosis and treatment of mild cognitive disorders may improve functioning and prevent the progression of brain disease. An understanding of the factors that impact neuronal loss, dendritic damage, and synaptic damage is important to the development of neuroprotective agents in the treatment of HAD, and to design new therapies for HAD-related psychiatric symptoms.

Material and methods

Subjects

Eight male rhesus monkeys (*Macaca mulatta*) of Indian origin were used in this study. The monkeys were herpes B virus negative, specific pathogenfree (SPF), from the same colony, approximately the same age (4 to 5 years), and all were raised under the same conditions. Animals were individually housed following Animal Biosafety Level 2 criteria in an American Association for Accreditation of Laboratory Animal Care (AAALAC) accredited facility. All work involving these monkeys conformed to the procedures outlined in the *Guide for the Care and Use of Laboratory Animals* published by the U.S. Department of Health and Human Services, National Institutes of Health. These animals were behaviorally trained, infected with neurotropic strains of SIV_{mac}, and subsequently euthanized following development of end stage simian AIDS. The behavioral test battery included measures of motor skill and cognitive function. Motor-, somatosensory-, auditory-, and visual-evoked potential were recorded 1 month prior to inoculation and every 4 to 6 weeks after inoculation. Five naïve monkeys served as controls for the evoked potentials and for stereological assessment.

Viral inoculation

Of the eight monkeys used in this study, four initially served as controls for a period of 6 months. The rest were inoculated by femoral bone marrow injection with two passaged strains of neurovirulent SIV_{mac}

(R71 and 17E). After the majority of the SIV-infected monkeys were euthanized, the four control monkeys were infected in the same way, with the same two virus strains. All animals received 0.5 ml of each viral homogenate (R71 and 17E) for a total volume of 1 ml that contained approximately 1000 $TCID_{50}$. All monkeys were monitored on a daily basis by the research and animal care staff for signs of illness.

Necropsy and histology

Monkeys were euthanized when one of the following criteria was met: weight loss exceeding 20% of body weight; inability to maintain an upright sitting posture; diarrhea unresponsive to therapy; severe loss of appetite; or failure to eat or drink for 2 consecutive days. Although five of the rapid progressors reached end-stage disease and met one of these criteria, one rapid progressor (AQ69) developed weakness and weight loss but died when recovering from anesthesia for an MRI. The two slow progressors developed somewhat different clinical signs, although both had some degree of weight loss. AQ15 was euthanized because of persistent bleeding from a skin tumor. At necropsy, this monkey was also found to have widely disseminated internal tumors and hepatitis. AQ94 was euthanized because of severe systemic illness (hepatitis, liver failure, wasting).

At necropsy, the animals were anesthetized with pentobarbital (10 mg/kg) given intravenously after initial ketamine tranquilization. In six of the SIV-infected animals and in all of the uninoculated control animals, brains were fixed by transcardial perfusion with 10% neutral-buffered formalin without saline perfusion. One of the infected macaques (AQ43) was not perfused with formalin so that fresh tissue samples could be taken for molecular analysis. Thereafter, in AQ43, saline was perfused through the aorta, and then the brain was removed and fixed immediately by immersion in 10% neutral-buffered formalin. The brain of AQ69 was fixed by immersion in 10% neutral-buffered formalin without perfusion. A complete postmortem examination was performed on each animal. Characteristic tissue morphology changes were used to assess the presence or absence of opportunistic infections.

All brains were bisected midsagittally, and the right hemispheres were used for neuropathological assessment using standard hematoxylin and eosin (H&E) staining of paraffin embedded tissue, sectioned at 5 μm (Raghavan *et al*, 1999). The left hemispheres were blocked in a standard coronal plane into a 38-mm-thick block and cryoprotected in 30% sucrose in 0.1 M phosphate buffer. The entire block was frozen-sectioned at 50 μm using a sliding microtome, yielding 640 to 700 sections. A 1 in 10 series of these sections was mounted and stained with 1% thionin. To visualize TH in the SN, sections were incubated free-floating in preblock solution (10% normal goat serum in phosphate-buffered saline (PBS)), washed, and incubated in primary antibody (TH rabbit polyclonal, 1:1000, Pel-Freez) overnight at room temperature. Sections were washed, incubated in biotinylated goat anti-mouse or anti-rabbit immunoglobulin G (IgG) diluted 1:200, washed, and incubated according to the protocol supplied by Vector Laboratories in their ABC Elite kit, and finally washed and reacted with 0.5% diaminobenzidine with 0.1% H_2O_2. They were then counterstained with 1% thionin.

Optical fractionator analysis

Globus pallidus: A subsample of sections that contained both the internal and external segments of the GP was selected. Beginning with a randomly selected start, every other slide was chosen for stereology. A 1-mm grid was placed at a random location over the GP on the backside of each slide in which the nucleus was present, and counts were made at the intersections of the grid bars. A 100× objective, NA 1.35, was used to obtain a thin focal plane through the sections for these studies. Neurons were counted when perikaryal cytoplasm first appeared in focus using an optical disector of 49 μm × 49 μm × 10 μm. The total section thickness was measured at each location. Neuron numbers were then calculated by the formula:

$$N = \Sigma Q^{-} = (1/ssf)(1/asf)(t/h)$$

where ΣQ^{-} = total cells counted; ssf = section sampling fraction (1 in 20); asf = area sampling fraction (obtained by comparing the area of the counting frame to the 1 mm sample spacing); t = mean section thickness (about 20 μm); and h = height of counting frame (10 μm). The coefficient of error (CE) was calculated as described in (West *et al*, 1991). The CE is a measure of the precision of the unbiased estimates of volume and neuron number for each structure examined. Sampling error was maintained at a low level, as evidence by CE estimates of 0.11 or less for all sections (Table 3). Thus, the values for volume and neuron number derived from the count of a sample of approximately 10 sections per animal have yielded a very accurate, unbiased estimate of the values for the whole structure. Volume of the nucleus was estimated using stereological probes for point counting and the application of Cavalieri's principle, which used the total number of 1-mm grid intersections overlying each region of the nucleus as the point count (Gundersen *et al*, 1988). We followed the criteria for differentiating between neurons and glia described by (Suner and Rakic, 1996); cells were considered neurons if they had round or smooth nuclei, the presence of nucleoli was observed, and cell body size was considerably larger in neurons than glia.

Substantia nigra: Estimates of total cell number were made on systematic-random sections through the SN. TH-immunopositive cells were counted using a computerized hardware-software system (StereoInvestigator, Colchester, VT) on TH-immunostained

Table 3 Coefficients of error for globus pallidus and substantia nigra

	SIV-infected monkeys							
	AQ70	*AQ69*	*AQ43*	*AQ12*	*AQ38*	*AQ20*	*AQ15*	*AQ94*
CEs for GP volume	0.023	0.010	0.022	0.020	0.020	0.017	0.019	0.019
CEs for GP neuron number	0.060	0.063	0.081	0.055	0.099	0.072	0.060	0.055
CEs for SN volume	0.083	0.079	0.060	NA	0.053	0.046	0.048	0.060
CEs for SN neuron number	0.050	0.110	0.060	NA	0.090	0.050	0.090	0.060

	Control monkeys				
	V	*W*	*X*	*Y*	*Z*
CEs for GP volume	0.018	0.022	0.019	0.019	0.020
CEs for GP neuron number	0.048	0.054	0.043	0.040	0.054
CEs for SN volume	0.057	0.055	0.053	0.038	0.043
CEs for SN neuron number	0.060	0.060	0.040	0.090	0.090

NA = not available.

sections counterstained with Nissl. Sampling error was 0.15 or less for all estimates (Table 3).

Neuropathological analysis

Alternating serial sections through the entire GP and SN were initially examined at 4× magnification. Each layer was then carefully evaluated at 10× and higher for the presence of perivascular cuffing, multinucleated giant cells, and microglial nodules. Cases were compared according to the quality and quantity of these features for an overall relative grade of 0 to 4 in the GP. Changes in the SN were less severe than in the GP; the same grading scale was used in the SN, but all severity values were within the 0 to 2 range. The number and size of microglial nodules in each case was the primary determinant of overall pathologic severity. It should be noted that the neuropathological analyses in this study were performed separately and are different from those presented in Raghavan *et al*, 1999, even though the same animals were examined in both studies.

In addition to the quantitative analysis of classic neuropathology, we also observed a very prominent, progressive change in neuronal morphology in the rapid progressors. For the animals in which there was more severe neuropathology, we noted changes such as retracted dendrites, complete loss of dendrites, and an alteration of soma shape. We were not able to assess the severity of these changes quantitatively in this study, but felt it was an important enough observation to discuss along with the other neuropathological findings, as these alterations in neuronal morphology were not found in the normal brain tissue of the control animals.

Neurological analysis

Ataxia, tremor, and weakness were determined by daily observation before and during behavioral testing, and as seen in weekly home cage behavior tapes. In addition, periodic neurological evaluations were performed, in which grip strength, gait, and climbing ability were assessed qualitatively. Disturbance

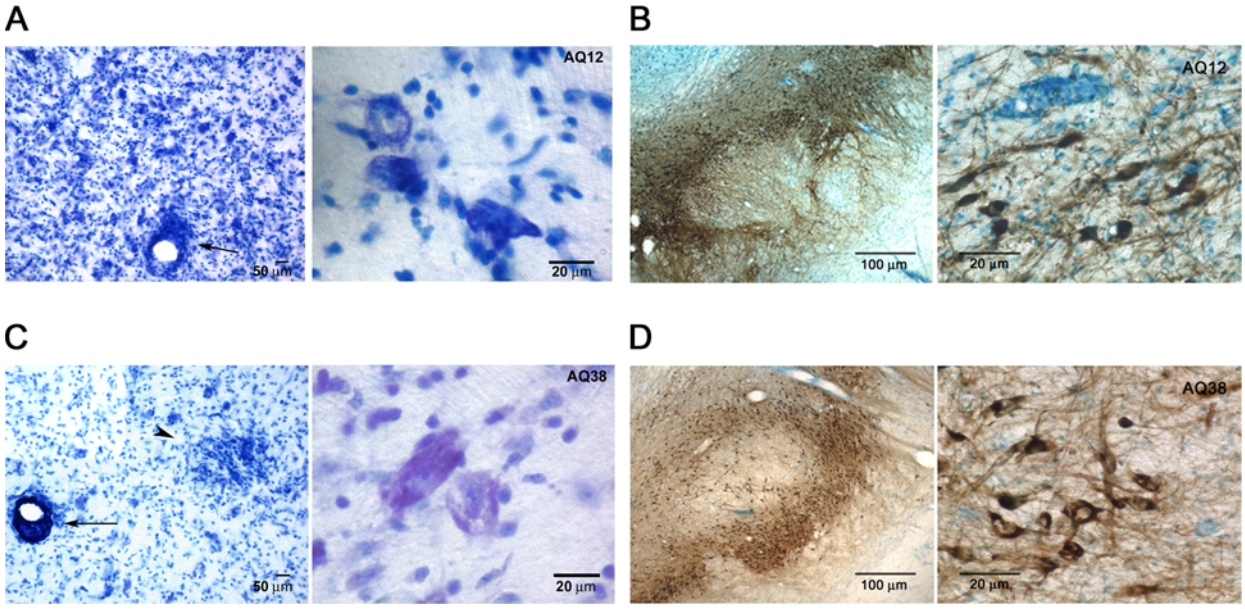

Figure 3 Examples of abnormal neuronal morphology in AQ12 and AQ38. In each row, the panel from the GP and the panel from the SN are from the same animal. *Left column*: Thionin-stained sections from the GP. Both AQ12 (**A**) and AQ38 (**C**) exhibit very heavy perivascular cuffing (*arrow*), numerous inflammatory foci (*arrow head*), and microglial nodules. Multinucleated giant cells were also observed (not shown). In addition, both animals clearly show a loss of dendrites, a rounding of the soma, and a lack of staining in the cytoplasm. *Right column*: Thionin- and tyrosine hydroxylase (TH)-stained sections from the SN. Both AQ12 (**B**) and AQ38 (**D**) exhibit misshapen cell bodies and a decrease in the density of the terminal field.

in gait, problems climbing, and lateralization of function in grooming and other "typical" primate activities were considered and used to determine the relative severity of ataxia, which was rated on a scale of 0 to 4. For an extensive discussion of the clinical symptoms observed and controls for "sickness behavior," see Marcario, 1999a, 1999b.

Statistical analyses

Descriptive statistics using means and standard deviations were computed for each group and each brain region. Differences between groups on each end point were tested using the Wilcoxon rank sum test, and a Kruskal-Wallis post hoc test. Because it was expected that the number of neurons could only decrease, and the control group would not be expected to demonstrate a change, one-sided tests for differences from control were used. For all other endpoints, two-sided tests were used. Only descriptive statistics were used for the slow progressors, because of the small number of animals in that group ($n = 2$).

Examination of the individual data on number of neurons revealed two apparent outliers—in the GP in monkey AQ12 and in the SN in monkey AQ38. Compared to all of the other animals, there was markedly less neuron loss than in the other rapid progressors. GP neuron counts for AQ12 were 1.9 standard deviations from the mean of the other monkeys in the group; SN neurons counts for AQ38 were 2.8 standard deviations from the mean of the other monkeys in that group. Statistical tests for detecting outliers have very low power for samples this small, and therefore these did not reach statistical significance for characterizing them as outliers. In both the GP of AQ12 and the SN of AQ38, there were morphological abnormalities, such as a lack of dendrites, abnormal soma shape, and lack of staining in the cytoplasm (Figure 3). So, even though the neurons in these animals met the stereological criteria to be counted as viable neurons (presence of an intact cell membrane and a nucleus), they were highly abnormal morphologically. Therefore, it was decided that the analyses would be performed both with and without these data, and both analyses are presented.

Pearson correlation coefficients (ρ) were calculated based on severity ratings (1 = none to very mild; 2 = mild; 3 = moderate; 4 = severe; 5 = very severe) for the number of weeks survived, motor-evoked potential changes, motor system neuropathology, GP neuropathology, GP neuron loss, SN neuropathology, and SN DA-containing neuron loss using the data from all six rapid progressors and both slow progressors (see Table 2).

References

An SF, Giometto B, Groves M, Miller RF, Beckett AA, Gray F, Tavolato B, Scaravilli F (1997). Axonal damage revealed by accumulation of beta-APP in HIV-positive individuals without AIDS. *J Neuropathol Exp Neurol* **56:** 1262–1268.

Arendt G, Hefter H, Elsing C, Strohmeyer G, Freund HJ (1990). Motor dysfunction in HIV-infected patients without clinically detectable central-nervous deficit. *J Neurol* **237:** 362–368.

Arendt G, Hefter H, Hilperath F, von Giesen HJ, Strohmeyer G, Freund HJ (1994). Motor analysis predicts progression in HIV-associated brain disease. *J Neurol Sci* **123:** 180–185.

Arendt G, Hefter H, Neuen-Jacob E, Wist S, Kuhlmann H, Strohmeyer G, Freund HJ (1993). Electrophysiological motor testing, MRI findings and clinical course in AIDS patients with dementia. *J Neurol* **240:** 439–445.

Aylward EH, Henderer JD, McArthur JC, Brettschneider PD, Harris GJ, Barta PE, Pearlson GD (1993). Reduced basal ganglia volume in HIV-1-associated dementia: results from quantitative neuroimaging. *Neurology* **43:** 2099–2104.

Bansal AK, Mactutus CF, Nath A, Maragos W, Hauser KF, Booze RM (2000). Neurotoxicity of HIV-1 proteins gp120 and Tat in the rat striatum. *Brain Res* **879:** 42–49.

Berger JR, Nath A (1997). HIV dementia and the basal ganglia. *Intervirology* **40:** 122–131.

Everall I, Barnes H, Spargo E, Lantos P (1995). Assessment of neuronal density in the putamen in human immunodeficiency virus (HIV) infection. Application of stereology and spatial analysis of quadrants. *J NeuroVirol* **1:** 126–129.

Everall IP, Glass JD, McArthur J, Spargo E, Lantos P (1994). Neuronal density in the superior frontal and temporal gyri does not correlate with the degree of human immunodeficiency virus-associated dementia. *Acta Neuropathol* **88:** 538–544.

Everall IP, Heaton RK, Marcotte TD, Ellis RJ, McCutchan JA, Atkinson JH, Grant I, Mallory M, Masliah E (1999). Cortical synaptic density is reduced in mild to moderate human immunodeficiency virus neurocognitive disorder. HNRC Group. HIV Neurobehavioral Research Center. *Brain Pathol* **9:** 209–217.

Everall IP, Luthert PJ, Lantos PL (1991). Neuronal loss in the frontal cortex in HIV infection. *Lancet* **337:** 1119–1121.

Fischer CP, Jorgen GGH, Pakkenberg B (1999). Preferential loss of large neocortical neurons during HIV infection: a study of the size distribution of neocortical neurons in the human brain. *Brain Res* **828:** 119–126.

Glass JD, Wesselingh SL, Selnes OA, McArthur JC (1993). Clinical-neuropathologic correlation in HIV-associated dementia [see comments]. *Neurology* **43:** 2230–2237.

Gonzalez RG, Cheng LL, Westmoreland SV, Sakaie KE, Becerra LR, Lee PL, Masliah E, Lackner AA (2000). Early brain injury in the SIV-macaque model of AIDS. *AIDS* **14:** 2841–2849.

Grant I, Heaton RK, Atkinson JH, Group H (1995). Neurocognitive disorders in HIV-1 infection. *Curr Top Microbiol Immunol* **202:** 11–32.

Gundersen HJ, Bendtsen TF, Korbo L, Marcussen N, Moller A, Nielsen K, Nyengaard JR, Pakkenberg B, Sorensen FB, Vesterby A, *et al* (1988). Some new, simple and efficient stereological methods and their use

in pathological research and diagnosis. *Apmis* **96:** 379–394.

Itoh K, Mehraein P, Weis S (2000). Neuronal damage of the substantia nigra in HIV-1 infected brains. *Acta Neuropathol (Berl)* **99:** 376–384.

Janssen RS, Cornblath DR, Epstein LG, Foa RP, McArthur JC, Price RW, *et al* (1991). Nomenclature and research case definitions for neurologic manifestations of human immunodeficiency virus-type 1 (HIV-1) infection. Report of a Working Group of the American Academy of Neurology AIDS Task Force. *Neurology* **41:** 778–785.

Ketzler S, Weis S, Haug H, Budka H (1990). Loss of neurons in the frontal cortex in AIDS brains. *Acta Neuropathol (Berl)* **80:** 92–94.

Li Q, Eiden LE, Cavert W, Reinhart TA, Rausch DM, Murray EA, Weihe E, Haase AT (1999). Increased expression of nitric oxide synthase and dendritic injury in simian immunodeficiency virus encephalitis. *J Hum Virol* **2:** 139–145.

Lopez OL, Smith G, Meltzer CC, Becker JT (1999). Dopamine systems in human immunodeficiency virus-associated dementia. *Neuropsychiatry Neuropsychol Behav Neurol* **12:** 184–192.

Mankowski JL, Queen SE, Tarwater PM, Fox KJ, Perry VH (2002). Accumulation of beta-amyloid precursor protein in axons correlates with CNS expression of SIV gp41. *J Neuropathol Exp Neurol* **61:** 85–90.

Marcario JK, Raymond LA, McKiernan BJ, Foresman LL, Joag SV, Raghavan R, Narayan O, Cheney PD (1999a). Motor skill impairment in SIV-infected rhesus macaques with rapidly and slowly progressing disease. *J Med Primatol* **28:** 105–117.

Marcario JK, Raymond LA, McKiernan BJ, Foresman LL, Joag SV, Raghavan R, Narayan O, Hershberger S, Cheney PD (1999b). Simple and choice reaction time performance in SIV-infected rhesus macaques. *AIDS Res Hum Retroviruses* **15:** 571–583.

Moglia A, Zandrini C, Alfonsi E, Rondanelli EG, Bono G, Nappi G (1991). Neurophysiological markers of central and peripheral involvement of the nervous system in HIV-infection. *Clin Electroencephalogr* **22:** 193–198.

Mouton PR (2002). *Principles and practices of unbiased stereology: an introduction for bioscientists*. Baltimore and London: The Johns Hopkins University Press.

Murray EA, Rausch DM, Lendvay J, Sharer LR, Eiden LE (1992). Cognitive and motor impairments associated with SIV infection in rhesus monkeys. *Science* **255:** 1246–1249.

Navia BA, Cho ES, Petito CK, Pricej RW (1986a). The AIDS dementia complex: II. Neuropathology. *Ann Neurol* **19:** 525–535.

Navia BA, Jordan BD, Price RW (1986b). The AIDS dementia complex: I. Clinical features. *Ann Neurol* **19:** 517–524.

Oster S, Christoffersen P, Gundersen HJ, Nielsen JO, Pakkenberg B, Pedersen C (1993). Cerebral atrophy in AIDS: a stereological study. *Acta Neuropathol (Berl)* **85:** 617–622.

Oster S, Christoffersen P, Gundersen HJ, Nielsen JO, Pedersen C, Pakkenberg B (1995). Six billion neurons lost in AIDS. A stereological study of the neocortex [published erratum appears in APMIS 1996 Jun;104(6):479]. *Apmis* **103:** 525–529.

Raghavan R, Cheney PD, Raymond LA, Joag SV, Stephens EB, Adany I, Pinson DM, Li Z, Marcario JK, Jia F, Wang C, Foresman L, Berman NE, Narayan O (1999). Morphological correlates of neurological dysfunction in macaques infected with neurovirulent simian immunodeficiency virus. *Neuropathol Appl Neurobiol* **25:** 285–294.

Raymond LA, Wallace D, Marcario JK, Raghavan R, Narayan O, Foresman LL, Berman NE, Cheney PD (1999). Motor evoked potentials in a rhesus macaque model of neuro-AIDS. *J NeuroVirol* **5:** 217–231.

Raymond LA, Wallace D, Raghavan R, Marcario JK, Johnson JK, Foresman LL, Joag SV, Narayan O, Berman NE, Cheney PD (2000). Sensory evoked potentials in SIV-infected monkeys with rapidly and slowly progressing disease. *AIDS Res Hum Retroviruses* **16:** 1163–1173.

Reyes MG, Faraldi F, Senseng CS, Flowers C, Fariello R (1991). Nigral degeneration in acquired immune deficiency syndrome (AIDS). *Acta Neuropathol (Berl)* **82:** 39–44.

Seilhean D, Duyckaerts C, Vazeux R, Bolgert F, Brunet P, Katlama C, Gentilini M, Hauw JJ (1993). HIV-1-associated cognitive/motor complex: absence of neuronal loss in the cerebral neocortex. *Neurology* **43:** 1492–1499.

Somma-Mauvais H, Farnarier G (1992). [Evoked potentials in HIV infection]. *Neurophysiol Clin* **22:** 369–384.

Subbiah P, Mouton P, Fedor H, McArthur JC, Glass JD (1996). Stereological analysis of cerebral atrophy in human immunodeficiency virus-associated dementia. *J Neuropathol Exp Neurol* **55:** 1032–1037.

Suner I, Rakic P (1996). Numerical relationship between neurons in the lateral geniculate nucleus and primary visual cortex in macaque monkeys. *Vis Neurosci* **13:** 585–590.

Weis S, Haug H, Budka H (1993). Neuronal damage in the cerebral cortex of AIDS brains: a morphometric study. *Acta Neuropathol (Berl)* **85:** 185–189.

West MJ, Slomianka L, Gundersen HJ (1991). Unbiased stereological estimation of the total number of neurons in the subdivisions of the rat hippocampus using the optical fractionator. *Anat Rec* **231:** 482–497.